Nonuniform Swelling of Alkali Swellable Microgels†

B. E. Rodriguez‡ and M. S. Wolfe*

DuPont Science and Engineering, P.O. Box 80356, Wilmington, Delaware 19880-0356

M. Fryd

DuPont Automotive Products, 3401 Grays Ferry Avenue, Philadelphia, Pennsylvania 19146

Received January 21, 1993; Revised Manuscript Received June 27, 1994®

ABSTRACT: Static and dynamic light scattering were used to study changes in the internal polymer segment density and particle swelling during the alkalization of aqueous dispersions of internally cross-linked, acid-containing latices (microgels). Upon neutralization, the microgels swell in excess of 200 times by volume, as evidenced by the measured hydrodynamic radius, R_h. Pronounced negative deviations of the ratio of the radius of gyration, R_g, to R_h, from the known value for homogeneous spheres along with curvature in Guinier plots of the angular dependent light scattering intensity indicate a nonuniform polymer segment density distribution within the microgels. Utilizing a simplistic core–shell model, we have determined the influence of the degree of neutralization, microgel cross-link density, and ionic strength on the nonuniform microgel swelling.

Introduction

During the alkalization of aqueous dispersions of carboxylic acid-containing latices the viscosity and shear thinning increase dramatically, making this class of materials useful for rheology control applications.[1,2] For example, Carbopols (B. F. Goodrich Co.) are cross-linked poly(acrylic acid) latices which are widely used as thickeners in cosmetics and pharmaceutical products.[3] Although the rheological properties of Carbopol and other high acid content latex dispersions have been investigated in some detail,[3-7] the mechanism for thickening of structurally well-defined alkali swellable latices has not been systematically examined.

The pronounced increase in viscosity and shear thinning upon neutralization has been attributed to the swelling of the latices which is caused by an increase in solubility and electrostatic repulsion between polymer chains.[8] In spite of the practical interest in carboxylic acid-containing latices, there have been few studies of the swelling mechanism and particle microstructure during alkalization,[9-12] and its relation to the dispersion structure and rheology.

Previous studies of the swelling of carboxylic acid-containing latices have focused mainly on uncross-linked particles that may have considerable dissolution, in addition to particle swelling, upon neutralization.[12,13] The resulting complex mixture of dissolved linear polymer and compositionally heterogeneous, swollen particles does not permit understanding of the dispersion structure and its influence on the rheology. With the acid content and its distribution within the latex being the key to swelling and dissolution, studies of the swelling[8-10] have concentrated on low acid content (2–3%), uncross-linked latices in which the acid is preferentially located at the latex surface. While the low acid content reduces dissolution, the latex composition is inhomogeneous and the desired feature for rheology control applications of dramatic swelling upon neutralization and, consequently, thickening is absent. As a first step toward understanding the dispersion structure–rheology relation for alkali swellable latices with high carboxylic acid content, it is the objective of the present study to determine the swelling behavior and structure of monodisperse, internally cross-linked, alkali swellable microgels as a function of the degree of neutralization, ionic strength, and cross-linker content.

With static and dynamic light scattering we have followed the microgel swelling during alkalization. Previously, for nonionized microgels dispersed in organic solvents, negative deviations of the ratio of the radius of gyration, R_g, to the hydrodynamic radius, R_h, from the value expected for homogeneous spheres have been attributed to nonuniform swelling.[14,15] This was rationalized in terms of a polymer segment density tail near the microgel surface due to dangling polymer chains comparable in molecular weight to the molecular weight between cross-links within the microgel interior. In the present study of alkali swellable microgels, we have observed much greater deviations from homogeneous sphere behavior. In addition, a physical interpretation of the nonuniform swelling in terms of a core–shell model for the angular dependence of the light scattering has been proposed.

Experimental Section

Microgel dispersions of ethyl acrylate (EA), methacrylic acid (MAA), and the cross-linker 1,4-butanediol diacrylate (BDDA) were prepared by conventional semicontinuous emulsion polymerization. This polymerization procedure (starved feed) was chosen to favor a homogeneous distribution of monomers within the microgel.[16] The compositions of the monomer emulsion feed for the two microgels A and B were 66/33/1 and 65/33/2 (EA/MAA/BDDA) by weight, respectively.

A typical synthetic procedure is as follows. A solution of 10.8 g of sodium lauryl sulfate (Duponol) in 3073 g of deionized water was stirred and heated to 80 °C while being purged with nitrogen. At this point 12.5% of the total monomer mixture, consisting of 882 g of EA, 441 g of MAA, and 13.4 g of BDDA, was added followed immediately by 18.2 g of a 7% dipotassium hydrogen phosphate solution and 20.2 g of a 5% ammonium persulfate solution (in deionized water). The reaction mixture exothermed and was stirred until the temperature leveled out at 85 °C. Maintaining the temperature at 85 °C, the remaining monomer mixture was added over 90 min. At that point, additional initiator was then added (18 g of 3% ammonium persulfate solution), and the temperature was maintained at 85 °C for an additional 2 h.

The microgels were cleaned with MilliQ (Millipore Co.) ultrapure water (resistivity = 18 MΩ cm) using the serum replacement method[17] to remove surfactant, unreacted monomers, and residual initiator. The microgels were considered clean when

† Contribution No. 6445.

‡ Permanent address: DuPont Automotive Products, 3401 Grays Ferry Avenue, Philadelphia, PA 19146.

® Abstract published in *Advance ACS Abstracts*, September 1, 1994.

0024-9297/94/2227-6642$04.50/0

the eluent had the same conductivity as the starting water. Although a small amount of uncross-linked polymer was extracted from the microgels when neutralized with base, as determined by separation by ultracentrifugation, its contribution to the light scattering intensity was found to not be significant and experiments were conducted without further cleaning. Dissolution of CO_2 was prevented by degassing the water and purging the samples with argon. The microgels were neutralized by the addition of 0.01 M NaOH to the dispersion.

The light scattering apparatus and procedures have been described elsewhere.[14] The average intensity of the scattered light was measured for scattering angles from 30 to 130° and converted to the Rayleigh ratio, R_{vv}, using toluene as a standard. The radius of gyration of the microgel, R_g, was determined from the slope at small q of a plot of the log of the Rayleigh ratio vs q^2 according to the Guinier approximation:[18]

$$R_{vv} \propto \exp(-q^2 R_g^2/3) \tag{1}$$

where $q = 4\pi n/\lambda \sin(\theta/2)$ is the scattering vector, n is the refractive index of the solvent, λ is the wavelength of the light (514.5 nm), and θ is the scattering angle. Due to curvature of some of the Guinier plots, the curves were fitted to a polynomial in order to obtain the initial slope ($-R_g^2/3$) required for the calculation of R_g. Second- and third-order polynomials were both found to fit all the curves within experimental error, giving the same calculated values of R_g. The apparent diffusion coefficient, D_{app}, and the apparent normalized second cumulant, $\delta_{z\,app}$, an indication of polydispersity in the diffusion coefficient, were calculated from the measured intensity autocorrelation function using the method of cumulants;[19-21] the z-average diffusion coefficient, D_z, and normalized second cumulant, δ_z, were obtained from extrapolation of D_{app} and $\delta_{z\,app}$ to $q = 0$, respectively. The hydrodynamic radius of the microgels was then calculated from D_z using the Stokes–Einstein relationship

$$D_z = k_B T/6\pi\eta_s R_h \tag{2}$$

where k_B is the Boltzmann constant, T is the absolute temperature, and η_s is the solvent viscosity. All measurements were performed at 25 °C.

Core–Shell Model

For colloidal dispersions or polymer solutions which are sufficiently dilute such that interparticle interactions are negligible, the scattering vector dependence of the light scattering intensity is given by the form factor $P(q)$. For particles with spherical symmetry $P(q)$ and R_g are given by[22]

$$P(q) = \frac{\int_0^\infty 4\pi r^2 \rho(r) \frac{\sin qr}{qr}\,dr}{\int_0^\infty 4\pi\rho(r) r^2\,dr} \tag{3}$$

$$R_g^2 = \frac{\int_0^\infty 4\pi r^4 \rho(r)\,dr}{\int_0^\infty 4\pi r^2 \rho(r)\,dr} \tag{4}$$

where $\rho(r)$ is the polymer density at r. For a polymer particle composed of two concentric spheres, i.e. a core–shell particle, having radii R and δR ($0 < \delta < 1$) and a polymer density defined by (Figure 1)

$$\rho(r) = 1 \quad 0 < r < \delta R$$

$$\rho(r) = \gamma \quad \delta R < r < R$$

$$\rho(r) = 0 \quad R < r \tag{5}$$

the form factor and radius of gyration are given by

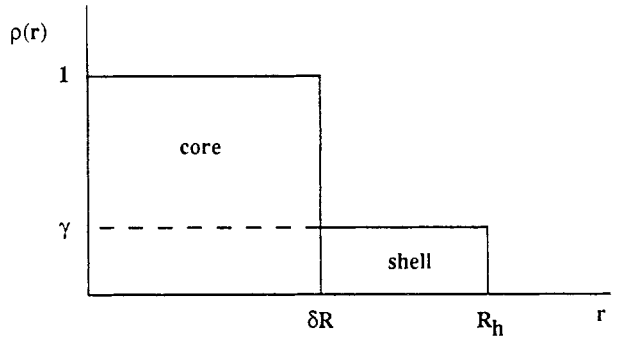

Figure 1. Normalized polymer density for idealized core–shell microgels. r is the distance from the center of the particle, δR is the radius of the core, and $R_{core+shell}$ is the total radius of the microgel.

$$P(q) = \left\{\frac{(1-\gamma)\delta^3 G(q\delta R) + \gamma G(qR)}{[\delta^3 + \gamma(1-\delta^3)]}\right\}^2 \tag{6}$$

and

$$R_g^2 = \frac{(3/5)R^2[\delta^5 + \gamma(1-\delta^5)]}{[\delta^3 + \gamma(1-\delta^3)]} \tag{7}$$

where

$$G(\upsilon) = \frac{3}{\upsilon^3}(\sin\upsilon - \upsilon\cos\upsilon) \tag{8}$$

Results and Discussion

The effect of the degree of neutralization on the pH of the microgel dispersion is shown in Figure 2. Samples were allowed to equilibrate at room temperature for 24 h prior to pH measurements. The degree of neutralization, which denotes the ratio $[OH^-]/[COOH] \times 100$, was calculated from the added base by assuming all of the acid initially present in the emulsion was incorporated into the microgels. The fact that the equivalence point roughly corresponds to 100% neutralization indicates that this is a reasonable assumption. Moreover, it indicates that all of the acid groups are readily accessible for titration within the equilibration time.

Static and dynamic light scattering were used to investigate the swelling behavior and microgel structure. However, since the microgels are polyelectrolytes with potentially strong interparticle interactions, it is necessary to ensure that the concentration of the microgels is sufficiently low that interparticle interactions do not affect the light scattering results. Figure 3 allows a determination of what constitutes a sufficiently low concentration for the static light scattering intensity. At concentrations for which interparticle interactions are negligible, R_{vv} will be proportional to concentration. Figure 3 demonstrates that this is clearly not the case at concentrations greater than 0.2%. At high concentrations, a reduction in R_{vv}/c (c is concentration) at small q indicates an increase in osmotic compressibility due to the presence of repulsive interparticle interactions.[23] In addition the presence of a maximum in R_{vv} as a function of q indicates a liquid-like interparticle ordering of the microgels with an interparticle separation distance comparable to $1/q$.[23] With decreasing concentration, a limiting behavior given by the solid curve is being approached. This solid curve represents those data at concentrations of 0.002, 0.005, 0.01, and 0.05 wt %. For clarity, only a single curve is shown. However, for concentrations less than 0.05 wt %, the magnitude of R_{vv}/c

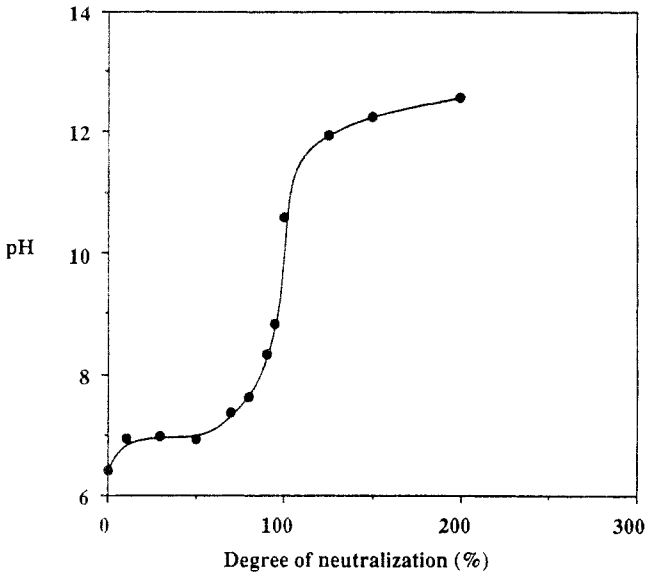

Figure 2. Titration curve for microgel A. Concentration = 0.5 wt %.

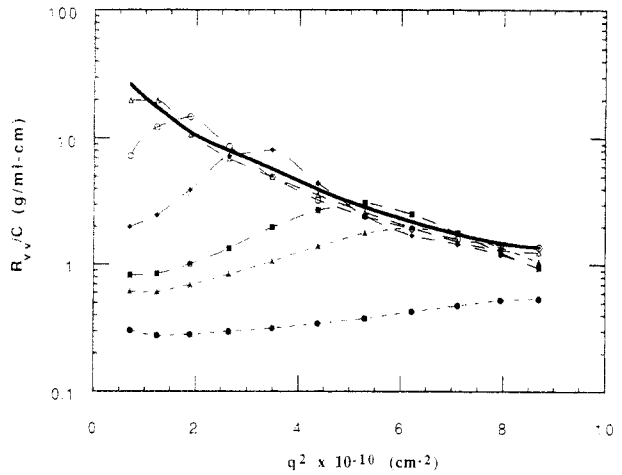

Figure 3. R_{vv}/c as a function of q^2 for microgel A at 100% neutralization. Concentrations (wt %): (●) 2.0; (▲) 1.0; (■) 0.8; (♦) 0.4; (○) 0.2; (△) 0.1. Dashed lines are to guide the eye. For clarity, the solid line represents data at 0.002, 0.005, 0.01, and 0.05 wt %.

as well as its q dependence is independent of concentration, indicating that interparticle interactions do not perturb the light scattering intensity.

The lack of interparticle interactions for concentrations less than 0.05% was also demonstrated for the dynamic light scattering, as shown in Figure 4. Here, R_h and δ_z are shown to be independent of concentration in this region. Having established the upper limit in concentration for which scattering contributions are only intramolecular in nature, concentrations 1 order of magnitude below this limit (≤0.005%) were utilized for the results presented below.

Guinier plots for dilute microgel dispersions are shown in Figure 5 at different degrees of neutralization. For clarity, not all of the measurements are included. At low degrees of neutralization the Guinier plots are linear and the radius of gyration is calculated from the slope according to eq 1. At high degrees of neutralization significant curvature is observed. To obtain the slope at small q needed for the calculation of R_g, the Guinier plots were fit to a second-order polynomial as discussed above. Curvature in the Guinier plots may be attributed to size polydispersity, to scattering from a particle comparable

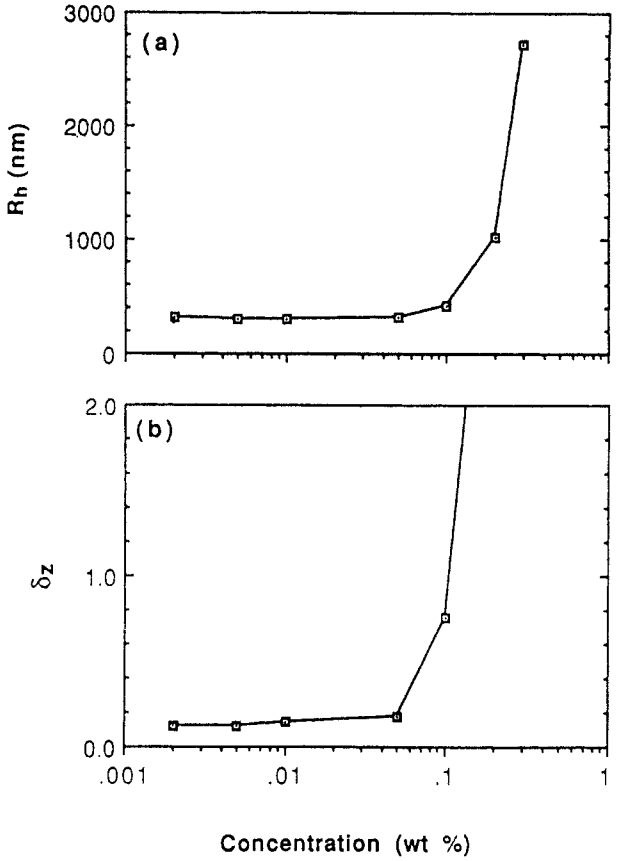

Figure 4. Hydrodynamic radius (a) and the normalized second cumulant (b) as a function of microgel concentration at 100% neutralization.

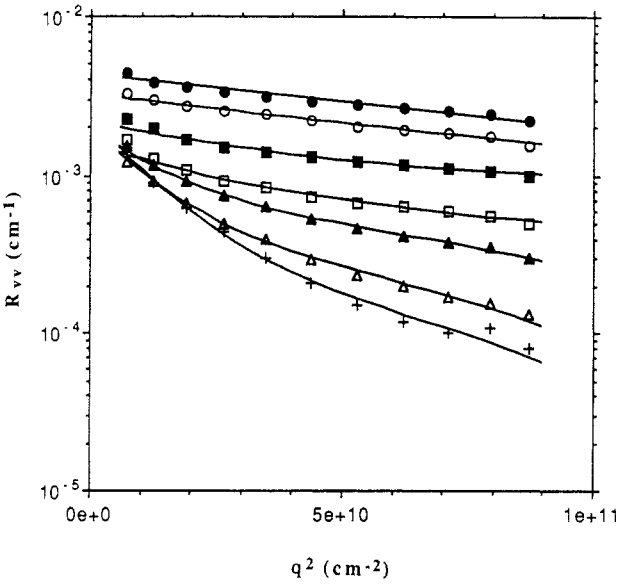

Figure 5. Guinier plots for a dilute dispersion of microgel A (concentration = 0.005 wt %). Degree of neutralization (%): (●) 0; (○) 30; (■) 40; (□) 50; (▲) 60; (△) 70; (+) 100. Lines are fits to the core–shell model (eq 6) as discussed in the text.

in size to q^{-1}, or to a nonuniform internal structure of the microgels.

When dispersed in swelling media in which electrostatic interparticle interactions are reduced, such as better than Θ organic solvents or water when neutralized at high ionic strength, the microgels display linear Guinier plots (Figure 6). The linearity of these plots suggests that size polydispersity is not significant and that swelling in these media is relatively uniform. Assuming microgel aggregation does not occur, size polydispersity is inherent to the sample

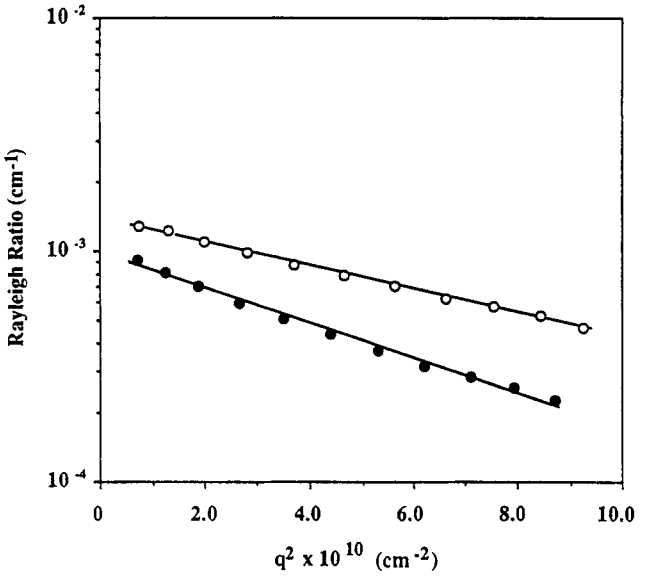

Figure 6. Guinier plots for microgel A dispersed in 2-propanol (○) and 0.9 M NaCl (●).

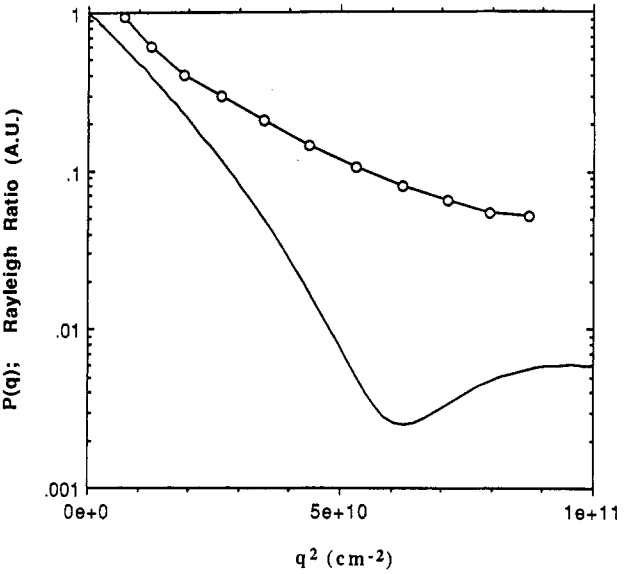

Figure 7. (Line without points) form factor for a trimodal distribution of homogeneous spheres. Equation 6 ($\gamma = 0$ and $\delta = 1$) was used to calculate the form factors for spheres with radii of 168, 187, and 206 nm which were summed (equal weightings) and normalized to 1 at $q = 0$. (Points) R_{vv} for microgel A (c = 0.005 wt %; 100% neutralization) in arbitrary units.

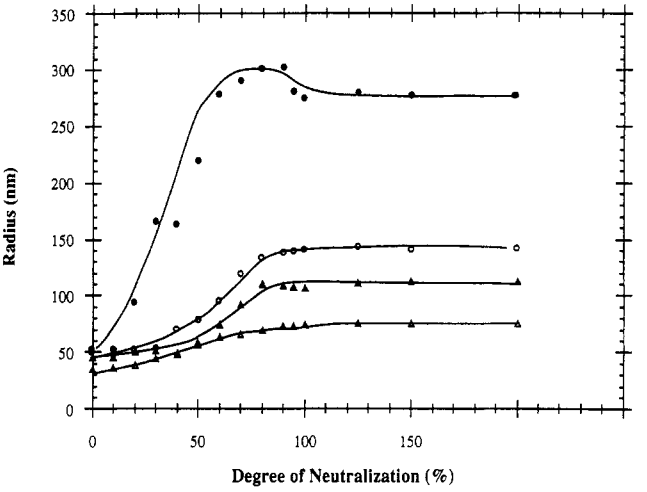

Figure 8. Dependence of the microgel radius on the degree of neutralization and cross-linker content. Symbols are as follows. Microgel A: (○) R_g; (●) R_h. Microgel B: (△) R_g; (▲) R_h.

and independent of the dispersing media. Therefore, these results suggest that size polydispersity is not significant. In addition, as will be discussed below, the ratio R_g/R_h is very close to that for a homogeneous sphere (~0.775).[24] Polydispersity would result in positive deviations from this value.[21]

The behavior of the normalized second cumulant also indicates that changes in the state of microgel aggregation do not occur as a function of the degree of neutralization. From the dynamic light scattering, δ_2 is indicative of changes in polydispersity. If aggregation occurs, it is unlikely that the polydispersity will not change. Within experimental error, from 0 to 100% neutralization, the normalized second cumulant is constant ($\delta_2 \sim 0.12$) within 20%, indicating no large changes in polydispersity or state of aggregation with neutralization.

Finally, the curvature in the Guinier plots cannot be explained by the form factor for scattering from a homogeneous spherical particle comparable in size to $1/q$. This form factor is given by eq 6 in the limit of no shell ($\gamma = 0$ and $\delta = 1$). For monodisperse homogeneous spheres, the form factor will have highly pronounced minima which are not observed in Figure 5. Introducing polydispersity will make the minima less pronounced. As an example, this is shown in Figure 7 for a trimodal distribution (187 nm radius, 10% smaller and 10% larger) in comparison with a 100% neutralization microgel. Although the initial slopes and calculated R_g's are similar, the shapes of the curves are very different. Unless an unrealistically high level of very small spheres is included, the form factor for polydisperse homogeneous spheres cannot explain the observed microgel Guinier plots. Therefore, the curvature in the Guinier plots for the microgels neutralized in water must be due to the internal microstructure of the microgels in water.

A large microgel swelling, as measured by the increase in both R_g and R_h, is observed as the degree of neutralization increases, as shown in Figure 8. At high degrees of neutralization the microgels increase their original volume by orders of magnitude. As expected, with increasing cross-linker content, the swelling decreases. Qualitatively, the microgel swelling can be understood in terms of changes in solubility of the constituent polymer as a function of the degree of neutralization. Unneutralized, the polymer is insoluble in water and therefore unswollen. With the increasing degree of neutralization, swelling of the microgels occurs due to the increasing MAA ionization and consequent improved solvent quality. This is clearly evidenced by the disappearance of the initial milky white appearance of a concentrated microgel dispersion to a nearly transparent appearance with increasing degree of neutralization. At high degrees of neutralization counterions and free ions screen the charge on the polymer chains and no further swelling occurs.

It is observed that although R_g and R_h both increase with the increasing degree of neutralization, qualitatively, the trends with neutralization differ. This is not surprising since R_g is sensitive to the refractive index distribution (mass distribution) within the microgel while R_h is sensitive to the hydrodynamics. The ratio of R_g/R_h is shown in Figure 9 for the more lightly cross-linked microgel A, with and without added salt. In comparison, for homogeneous, nondraining spheres, HS, this ratio is 0.775.[24] At high ionic strength, where electrostatic repulsions between ionized acid groups are suppressed resulting in a reduced swelling (Figure 10), only small negative deviations from

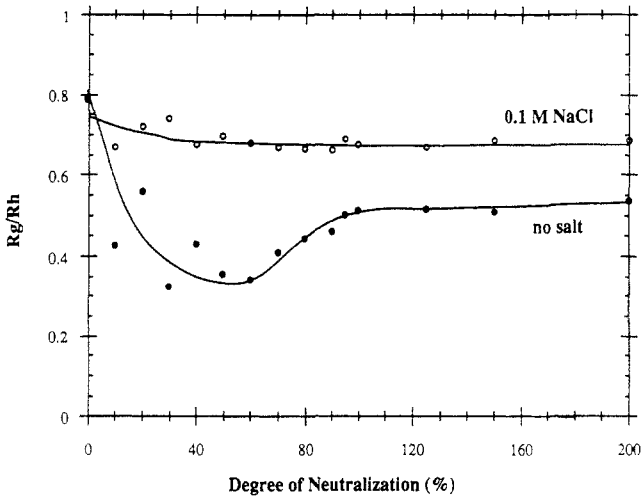

Figure 9. R_g/R_h for microgel A as a function of the degree of neutralization and added salt.

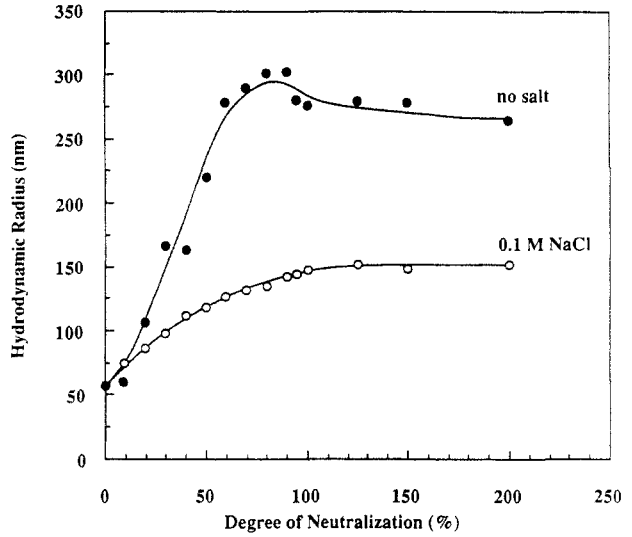

Figure 10. Hydrodynamic radius for microgel A as a function of the degree of neutralization and added salt.

the HS value occur with increasing neutralization. However, with no added salt the dependence of R_g/R_h is complex, going through a shallow minimum at approximately 50% neutralization. Only in the unneutralized and unswollen state is the HS value observed. In addition, it should be noted that polydispersity in size cannot explain these deviations since it would give rise to positive rather than negative deviations from the HS value.[21] Similar, but smaller, deviations for nonionized microgels in organic solvents were attributed to the nonuniform polymer segment density distribution within the microgels.[14,15] As illustrated in Figure 11, for a long polymeric tail near the microgel surface, although the tail represents a small fraction of the microgel mass and therefore makes only a small contribution to R_g, it strongly affects the hydrodynamics, resulting in a larger R_h. This combined effect results in a ratio of R_g to R_h smaller than the HS ratio.

To explain the nonuniform swelling, the microgels were modeled in terms of a core–shell structure. We have assumed they are composed of a cross-linked central core and an outer shell of dangling chains, with uniform polymer densities within each region (Figure 1). We have also assumed that the monomers are uniformly distributed within the microgel so that the refractive index increment is equal in both regions. That this is a reasonable assumption is based in part on the starved feed polymerization conditions[16] used for the microgel synthesis. This polymerization procedure tends to force the particle composition, as it grows radially, to be the instantaneous composition of the monomer feed which, in the present case, was uniform. In addition, from studies of dry microgel films, we have found only a single glass transition temperature and an absence of small angle X-ray scattering. These results suggest a lack of heterogeneity in the microgel structure. Finally, we have assumed that the total radius (core + shell) of the microgel is equal to the measured hydrodynamic radius; i.e., the microgels are nondraining. While the core–shell structure oversimplifies the internal microgel structure, it provides similar physical insight to that of a model with a more realistic internal microgel structure, but with a minimum of fitting parameters. Similarly, although the nondraining assumption may be incorrect for the highly swollen microgels, it is not expected to invalidate any of the qualitative trends presented below.

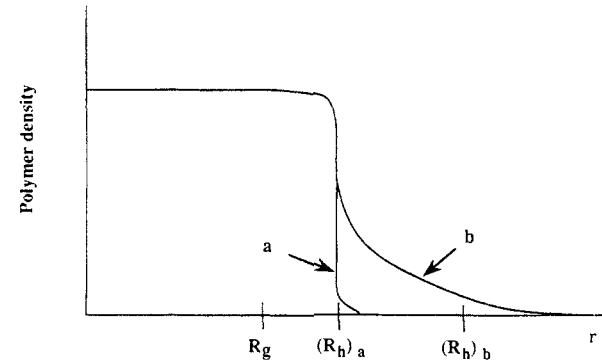

Figure 11. Hypothetical polymer density as a function of the distance form the microgel center: (a) uniform density; (b) long polymeric tail.

In dilute noninteracting systems the measured Rayleigh ratio, R_{vv}, is proportional to the form factor, $P(q)$, of the disperse particles. We have therefore used eq 6 to fit the experimental Rayleigh ratios by a least-squares procedure. Experimental points at the lowest scattering angle, which are most sensitive to any dust, were not included in the fitting procedure. The core radius, δR, and the normalized shell density, γ, were used as fitting parameters. Lines in Figure 5 are the best fits to the data. A good agreement between experimental and calculated values is obtained using this model.

To check the validity of the calculation of R_g from the angular dependence of the light scattering, as discussed above, R_g was also calculated utilizing the complete range of scattering angles with the core–shell model fitting parameters in eq 7. The resulting ratios of R_g to R_h shown in Figure 12 demonstrate the same trends with the degree of neutralization as those observed in Figure 9. Quantitative differences are not surprising due to the different empirical definitions of R_g.

For the core–shell model, Figures 13 and 14 show R_{core} (δR) and $R_{core+shell}$, and the polymer volume fraction within the core and shell, respectively, as a function of the degree of neutralization. These modeling results suggest that at low degrees of neutralization, only acid functionality near the microgel surface is ionized, resulting in swelling of the "shell", while the bulk of the acid functionality in the "core" remains unswollen until approximately 50% neutralization. With further increases in the degree of neutralization, the "core" also swells, however, to a much smaller extent. At 100% neutralization for example, the "core" and "shell" exhibit factors of 14 and 350 swelling by volume and microgel fractions of 95% and 5%, respectively. At higher

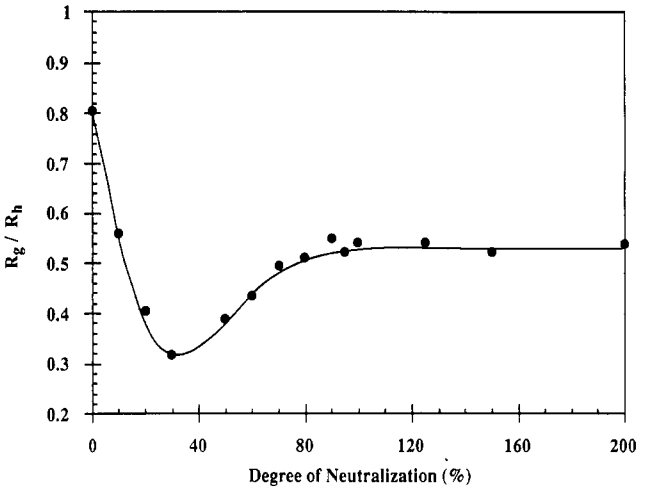

Figure 12. R_g/R_h as a function of the degree of neutralization. R_g was calculated using eq 7 as described in the text.

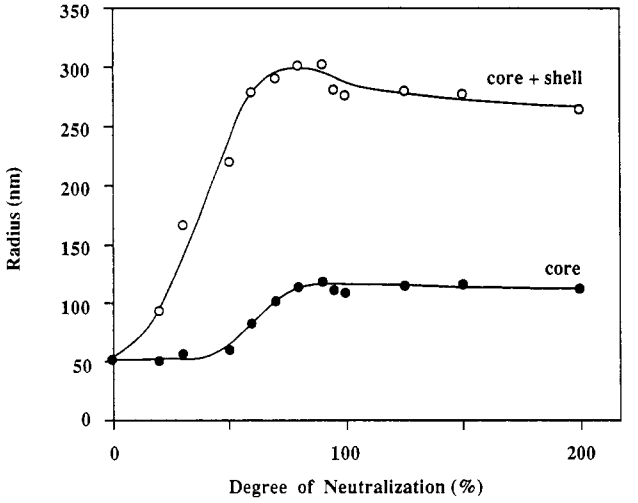

Figure 13. Dependence of the core radius and total microgel radius on the degree of neutralization.

degrees of neutralization while maintaining a pronounced nonuniform swelling, the nonuniformity decreases slightly due to ionic screening of the electrostatic repulsions between the carboxylate groups.

Conclusions

We have demonstrated that compositionally homogeneous alkali swellable microgels exhibit a pronounced nonuniform swelling when neutralized with base. This is evidenced by negative deviations of R_g/R_h from the value for homogeneous spheres as well as the curvature in Guinier plots of the light scattering intensity. The nonuniform swelling is a result of electrostatic repulsion between ionized carboxylic acid groups attached to polymer chains near the surface of the microgels. The nonuniform swelling becomes less pronounced with increasing ionic strength or microgel cross-linker content and can be quantitatively explained in terms of a core–shell model.

Acknowledgment. We thank J. England for his valuable assistance with the experiments and data analysis.

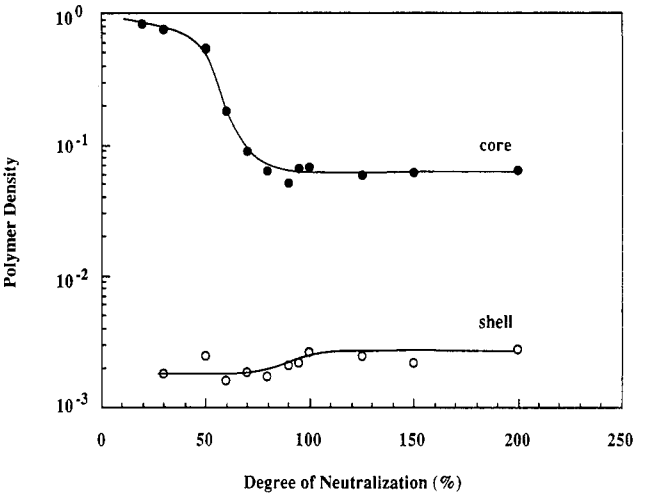

Figure 14. Effect of the degree of neutralization on the polymer density of the core and the shell.

References and Notes

(1) Shay, G. D. In *Polymers in Aqueous Media*; Glass, J. E., Ed.; American Chemical Society: Washington, DC, 1989.
(2) Quadrat, O.; Mrkvickova, L.; Jasna, E.; Snupareck, J., Jr. *Colloid Polym. Sci.* **1990**, *268*, 493, 921.
(3) Barry, B. W.; Meyer, M. C. *Int. J. Pharm.* **1979**, *2*, 1.
(4) Quadrat, O.; Snuparek, J., Jr. *Prog. Org. Coat.* **1990**, *18*, 207.
(5) Taylor, N. W.; Gordon, S. H. *J. Appl. Polym. Sci.* **1982**, *27*, 4377.
(6) Quadrat, O.; Mrkvickova, L.; Snuparek, J., Jr. *J. Colloid Interface Sci.* **1988**, *123* (2), 353.
(7) Ketz, R. J., Jr.; Prud'homme, R. K.; Graessley, W. W. *Rheol. Acta* **1988**, *27*, 531.
(8) Ford, J. R.; Morfesis, A. A.; Rowell, R. L. *J. Colloid Interface Sci.* **1985**, *105* (2), 516.
(9) Rowell, R. L.; Ford, J. R.; Parsons, J. W. In *Polymer Colloids II*; Fitch, R. M., Ed.; Plenum Press: New York, 1980; p 27.
(10) Ford, J. R.; Rowell, R. L.; Bassett, D. R. *ACS Symp. Ser.* **1981**, No. 165, 279.
(11) Bassett, D. R.; Hoy, K. L. In *Polymer Colloids II*; Fitch, R. M., Ed.; Plenum Press: New York, 1980; p 1.
(12) Verbrugge, C. J. *J. Appl. Polym. Sci.* **1970**, *14*, 897, 911.
(13) Muroi, S.; Hosoi, K.; Ishikawa, T. *J. Appl. Polym. Sci.* **1967**, *11*, 1963.
(14) Wolfe, M. S.; Scopazzi, C. *J. Colloid Interface Sci.* **1989**, *133* (1), 265.
(15) Rodriguez, B. E.; Kaler, E. W.; Wolfe, M. S. *Langmuir* **1992**, *8* (10), 2382.
(16) Nishida, S.; El-Aasser, M. S.; Klein, A.; Vanderhoff, J. W. *ACS Symp. Ser.* **1981**, No. 165, 291.
(17) Ahmed, S. M.; El-Aasser, M. S.; Pauli, G. H.; Poehlein, G. W.; Vanderhoff, J. W. *J. Colloid Interface Sci.* **1980**, *73*, 388.
(18) Guinier, A.; Fournet, G. *Small-Angle Scattering of X-rays*; Wiley: New York, 1955.
(19) Koppel, D. E. *J. Chem. Phys.* **1972**, *57*, 4814.
(20) Selser, J. C. *Macromolecules* **1979**, *12*, 909.
(21) King, T. A.; Treadaway, M. F. *J. Chem. Soc., Faraday Trans. 2* **1977**, *73*, 1616.
(22) Kerker, M. *The Scattering of Light, and other Electromagnetic Radiation*; Academic Press: New York, 1969.
(23) Nieuwenhuis, E. A.; Pathmanmanoharan, C.; Vrij, A. *J. Colloid Interface Sci.* **1981**, *81*, 196.
(24) Schmidt, M.; Nerger, D.; Burchard, W. *Polymer* **1979**, *20*, 581.